eNeuro

Research Article: New Research | *Cognition and Behavior*

Characterizing population EEG dynamics throughout adulthood

Abbreviated title: Population EEG Dynamics

Ali Hashemi[1], Lou J. Pino[2], Graeme Moffat[2], Karen J. Mathewson[1], Chris Aimone[2], Patrick J. Bennett[1], Louis A. Schmidt[1] and Allison B. Sekuler[1]

[1]*Department of Psychology, Neuroscience, & Behaviour, McMaster University, Hamilton, Ontario, L8S 4K1, CANADA*

[2]*InteraXon Inc., Toronto, Ontario, M5V 1K4, CANADA*

DOI: 10.1523/ENEURO.0275-16.2016

Received: 9 September 2016

Revised: 31 October 2016

Accepted: 16 November 2016

Published: 30 November 2016

Author contributions: AH, ABS, and LJP designed research. AH, LJP, KJM, LAS, and PJB analyzed data. LJP, GM, and CA contributed unpublished analytic tools. AH, KJM, LAS, ABS, and PJB wrote paper.

Funding: Natural Sciences and Engineering Research Council of Canada (Conseil de Recherches en Sciences Naturelles et en Génie du Canada)

Conflict of Interest: The authors AH, KJM, PJB, LAS, and ABS declare no competing financial interests. Authors LJP, GM, and CA are current employees of InteraXon, the creators of the Muse.

Natural Sciences and Engineering Research Council of Canada (Conseil de Recherches en Sciences Naturelles et en Génie du Canada).

Correspondence should be addressed to Ali Hashemi, Email: hashea@mcmaster.ca

Cite as: eNeuro 2016; 10.1523/ENEURO.0275-16.2016

Characterizing population EEG dynamics throughout adulthood

Abbreviated title: Population EEG Dynamics

Ali Hashemi[1], Lou J. Pino[2], Graeme Moffat[2], Karen J. Mathewson[1], Chris Aimone[2], Patrick J. Bennett[1], Louis A. Schmidt[1], & Allison B. Sekuler[1]

Affiliations

1. Department of Psychology, Neuroscience, & Behaviour, McMaster University, Hamilton, Ontario, L8S 4K1, CANADA
2. InteraXon Inc., Toronto, Ontario, M5V 1K4, CANADA

Correspondence should be addressed to Ali Hashemi (hashea@mcmaster.ca)

Author contributions

AH, ABS, and LJP designed research. AH, LJP, KJM, LAS, and PJB analyzed data. LJP, GM, and CA contributed unpublished analytic tools. AH, KJM, LAS, ABS, and PJB wrote paper.

Details

Number of pages 23
Number of figures: 9
Number of tables: 3

Number of words in title: 6
Number of characters in abbreviated title: 23
Number of words in abstract: 250
Number of words in introduction: 547
Number of words in discussion: 1788

Acknowledgements

Funding was provided by the National Science & Engineering Research Council (NSERC). Additional thanks goes to Javier Moreno for his help during data processing and data visualization.

Conflict of interest

The authors AH, KJM, PJB, LAS, and ABS declare no competing financial interests. Authors LJP, GM, and CA are current employees of InteraXon, the creators of the Muse.

Characterizing population EEG dynamics throughout adulthood

Ali Hashemi[1*], Lou J. Pino[2], Graeme Moffat[2], Karen J. Mathewson[1], Chris Aimone[2], Patrick J. Bennett[1], Louis A. Schmidt[1], and Allison B. Sekuler[1]

[*] *Corresponding author: Ali Hashemi (hashea@mcmaster.ca)*
[1] *Department of Psychology, Neuroscience, & Behaviour, McMaster University, Hamilton, Ontario, L8S 4K1, CANADA*
[2] *InteraXon Inc., Toronto, Ontario, M5V 1K4, CANADA*

Abstract

For decades, electroencephalography (EEG) has been a useful tool for investigating the neural mechanisms underlying human psychological processes. However, the amount of time needed to gather EEG data means that most laboratory studies use relatively small sample sizes. Using the Muse, a portable and wireless 4-channel EEG headband, we obtained EEG recordings from 6029 subjects who ranged from 18-88 years in age while they completed a category exemplar task followed by a meditation exercise. Here, we report age-related changes in EEG power at a fine chronological scale for delta, theta, alpha, and beta bands, as well as peak alpha frequency and alpha asymmetry measures for both frontal and temporoparietal sites. We found that EEG power changed as a function of age, and that the age-related changes depended on sex and frequency band. We found an overall age-related shift in band power from lower to higher frequencies, especially for females. We also found a gradual, year-by-year slowing of the peak alpha frequency with increasing age. Finally, our analysis of alpha asymmetry revealed greater relative right frontal activity. Our results replicate several previous age- and sex-related findings, and show how some previously-observed changes during childhood extend throughout the lifespan. Unlike previous age-related EEG studies which have been limited by sample size and restricted age ranges, our work highlights the advantage of using large, representative samples to address questions about developmental brain changes. We discuss our findings in terms of their relevance to attentional processes, and brain-based models of emotional well-being and aging.

Significance Statement

We collected over 6000 participants' EEG data during two different tasks in uncontrolled environments, and identified subtle but robust sex differences in several EEG measures, as well as age-related shifts in EEG activity on a year-by-year scale. Our large sample size provided us with the power to highlight gradual age-related changes in several EEG measures, and how those changes differ between males and females, in a representative population of individuals completing the tasks in uncontrolled, natural environments.

1 Introduction

For many decades, electroencephalography (EEG) has been used effectively for different purposes in a variety of fields. For example, clinicians have used EEG to understand several illnesses, including epilepsy and sleep disorders; engineers have used EEG to develop wheelchairs that respond to brain states; and psychologists have used EEG to track the temporal flow of information through the sensory systems and identify neural correlates of psychological processes. Although EEG has been a useful clinical and scientific tool, its applications have been constrained by the fact that recording of EEG data is time-consuming and requires laboratories equipped with expensive EEG equipment. Researchers typically collect data from a small sample of participants, and hope that other researchers replicate the results to validate inferences about the general population. Using much larger samples would, in most cases, make it easier to establish the robustness and generalizability of empirical findings.

Fortunately, recent technological advances and industry-led innovation have lead to the development of research-grade EEG products that are affordable and easily used by consumers. Our focus here is on the Muse, the EEG-headband created by InteraXon (Toronto, Canada), who commercialized it as a neurofeedback tool in mindfulness-based stress reduction (MBSR). MBSR-related benefits aside (see Kabat-Zinn (1994) for an explanation of MBSR and Kabat-Zinn (2003) and Davidson et al. (2003) for some empirical evidence of its benefits), arguably the most beneficial aspect of the Muse to researchers has been that the company has amassed hundreds of thousands of sessions of EEG data from over tens of thousands of consenting users, making InteraXon, to our knowledge, the holder of the largest EEG database in the world. Not only is the current database valuable and ripe for analysis, the ease of use and low cost of the Muse allows for wide-spread deployment of the hardware to capture EEG activity outside of the laboratory.

Consumer use of the Muse typically consists of pairing it with a compatible mobile device via Bluetooth technology, and using the Muse application to complete a breath-guided meditation session. During each session, users also complete a variation of the Category Exemplar Task which, in combination with the MBSR portion of the session, allows for the EEG to be captured for both a 'busy' mind during the task, and a 'calm' mind during the MBSR exercise. The Muse database consists of tagged EEG data representing electrocortical activity recorded at four scalp locations –

temporoparietal (TP9 and TP10) and frontal (AF7 and AF8) locations plus a fifth frontal electrode (Fpz) that is used as the reference – while participants complete the MBSR meditation session and the Category Exemplar Task.

Here, we used the data from thousands of users to study age-related changes in EEG power throughout adulthood. We report several changes as a function of age, including increased power in the alpha and beta bands, an age-related reduction in peak alpha frequency, and an overall rightward bias in frontal alpha asymmetry. We discuss the consistency of our findings with previous laboratory studies of attention regulation and other processes thought to be related to mindfulness meditation. We also discuss our findings in the framework of brain-based models of well-being related to aging, as well as the value of Big Data in EEG studies.

2 Methods

2.1 Participants

Data were collected from individuals who used the Muse between May 2014 and January 2015, and opted into the optional research program in the accompanying Muse/Calm mobile application. Our original clean database contained 6081 unique users, which then was reduced by excluding users who were below the age of 18 or who chose not to report their age, for a final count of 6029 individuals. The distribution of the age and gender of the users is displayed in Table 1.

Age (years)	Male	Female	Total
18-19	48	17	65
20-29	854	324	1178
30-39	1227	419	1646
40-49	1059	359	1418
50-59	708	344	1052
60-69	400	166	566
70-79	77	20	97
≥ 80	6	1	7
Total	4379	1650	6029

Table 1 – User and session distribution by age and sex. For each user, data were averaged for up to 5 sessions.

2.2 Design & Procedure

Data were collected using the Muse (formerly known as Calm) mobile application found on the Apple App Store, Google Play, and Amazon Appstore. At the beginning of each user's first session, the app provided visual and auditory instructions on how to apply the Muse headset to attain optimal signal quality, and general information about the Muse application which provides auditory feedback to assist in MBSR meditation. The auditory feedback resembled the natural sound of wind and ocean waves, with increasing sounds reflecting an active mind, and quietness reflecting a calm mind. The algorithm determining the auditory feedback involved an individual calibration step to establish a baseline. This calibration step was a one-minute phase in which participants completed a version of the Category Exemplar Task: participants were told to close their eyes, and at 0, 20, and 40 seconds were given a new category for which they were to think of as many examples as they could.

Following the calibration (CAL) procedure, the participant began a Neurofeedback (NFB) session. The default duration of the NFB session was three-minutes, but users could have opted to complete 3, 5, 10, or 20 minute sessions. During the NFB session, users were instructed to close their eyes and focus their mind on counting their breaths, and to silently/mentally acknowledge any deviations of attention from counting their breaths (i.e., mind-wandering), and refocus on counting their breathing. Although this may not be the traditional definition of NFB, we refer to this technique as NFB since the Muse software applies a trade-secret algorithm developed through machine learning to reward a decrease in EEG signatures of mind-wandering.

The amount of data varied significantly across users, with some individuals recording several hundred CAL and NFB sessions. To prevent our analyses from being biased by frequent users, we averaged the first several sessions, up to a maximum of five sessions, to create a single pair of averaged CAL and NFB sessions for each user.

2.3 EEG Recording & Processing

EEG data were recorded using InteraXon's Muse headset (RRID:SCR_014418). The Muse is a consumer and research-grade EEG headset with 4 recording channels (TP9, TP10, AF7, and AF8) referenced to a fifth channel located at Fpz. Active noise suppression was achieved by creating driven right leg (DRL) circuits between two forehead DRL channels and Fpz. The DRL circuits were used to establish that the electrodes have skin contact (i.e., any activity detected by the circuit indicated that the headset was positioned to have skin contact), after which the characteristics of the incoming EEG signal (variance, amplitude, and kurtosis) were used in a decision tree where low power, low amplitude, and low kurtosis were favored in classifying the real-time signal as clean. EEG was sampled at 220 Hz.

Data were collected from participants from several continents, and the appropriate 50 Hz (Europe and Asia) or 60 Hz (North America) notch filters were applied to each individual session depending on self-reported location. Artefacts were detected by first applying a 2-36 Hz band-pass filter on the raw EEG signal. Continuous EEG was then divided into 1.16 second (256 samples) epochs, and each epoch's overall power was compared to a threshold of 275 μV^2. The threshold was previously determined by large-scale visual inspection to separate clean and noisy data. Only epochs exceeding the threshold were rejected from the EEG session. If more than 10% of any session at any of the four channels was rejected using this method, then that entire session (NFB and CAL) was excluded from analysis. The database originally contained 139,548 sessions, but applying the rejection criteria above reduced that to 74,321 sessions (i.e., 47% of the sessions were rejected due to containing excessive artefacts). We further excluded all sessions beyond the first five clean sessions per user, reducing the database to 22,386 sessions, from 6029 unique users. There was an average of 3.7 sessions per user, with each user having at least 1 session but no more than 5 sessions.

2.4 EEG Measures

All analyses were done on EEG data from the entire cleaned session. For each session, Matlab's *fft* function was used compute a power spectrum with a frequency resolution of 1 Hz. Total power (μV^2) was calculated for the delta (δ, 0-2 Hz), theta (θ, 3-7 Hz), alpha (α, 8-13 Hz), and beta (β, 14-30 Hz) bands. Lower and upper alpha power were also quantified in the 8-10 and 11-13 Hz frequency ranges. Band power was then $\log_{10}$-transformed for normalization. Additionally, alpha asymmetry was calculated by subtracting the $\log_{10}$-transformed left alpha power from the $\log_{10}$-transformed right alpha power separately for the frontal and temporal locations. Lastly, alpha peak frequency, defined as the frequency component in the 8-13 Hz range with the highest power, was measured for each person, separately at each channel.

3 Results

Power spectra, averaged across users, were calculated separately for the CAL and NFB sessions at each channel (Figure 1). EEG power was greater in temporoparietal than frontal regions, especially at lower frequencies (Figure 1). There was also a very noticeable peak in the alpha frequency range in temporoparietal channels, but not frontal channels. Total power in the 0-30 Hz range was significantly higher in females than males at all channels (Figure 2). For CAL, the sex difference was significant at all channels (t_{6027}'s$> 5.08, p < 0.00001$). For NFB, the sex difference was significant at channels AF7, AF8, and TP10 (t_{6027}'s$> 3.4, p < 0.001$) but not at TP9 ($t_{6027} = 1.66, p = 0.097$).

3.1 Band analysis

To evaluate age-related changes in each dependent variable, we used linear models that included Age, Age^2, Sex, Task, and Channel, as well as all 2-, 3-, and 4-way interactions, as predictor variables. For all measures, Task and Channel each had at least one significant interaction with either each other, Age, Age^2, Sex, and/or the Age $\times$ Sex and Age^2 $\times$ Sex interaction. Due to these interactions, we proceeded with separate analyses for each channel and task, using linear models that included only Age, Age^2, Sex, and the Age $\times$ Sex and Age^2 $\times$ Sex interactions. If either interaction was significant, then separate models that included Age and Age^2 as predictors were fit to data from males and females. Although all analyses were conducted for both CAL and NFB, for brevity, we present the accompanying data figures only from the NFB session. The pattern of results were qualitatively similar across CAL and NFB except in a few cases which we discuss in the text. Furthermore, the Table 2 presents all of the results from the models fit to the CAL data. To view the accompanying figures for CAL sessions, please contact the corresponding author.

Preliminary analyses indicated that the average within-age variance (i.e., variance across all participants within the same year, averaged across all years) was much larger than the between-age variance – a trend seen across all channels for all measures (Figure 3). Because we were interested primarily in age-related variance, we used weighted least-squares (WLS) to fit linear models to the mean at each age, where the weight corresponded to the number of users at each age. This method effectively removes within-subject and within-age variation. The coefficients of the resulting WLS model are identical to a traditional least-squares regression applied to the non-averaged data from individual users, but the overall fit of the model (i.e., R^2) is much higher because the averaging removes within-age variance.

In all models, Age was treated as an integer variable and Sex (male=0; female=1) was a dichotomous variable. Furthermore, to have a more meaningful intercept in our model, Age was centered on the mean age of our participants (i.e., 42 years old). Therefore, the best-fitting value of the intercept represents the estimate of the dependent variable (e.g., delta power) for males at 42 years of age, the Sex parameter represents the difference between males and females at 42 years of age, the Age and Age^2 parameters represent the change in the dependent variable that occurs (on average) in males with each unit change in Age and Age^2, and the Sex $\times$ Age and Sex $\times$ Age^2 parameters represent the difference between the Age and Age^2 effects in males and females. The results of the regression analyses are shown in Tables 2 and 3. Due to the large sample size, the linear model accounted for a statistically significant portion of the variance in every case. However, for the sake of brevity our discussion focuses on the subset of cases in which the linear model accounted for at least 50% of the age-related variance.

Table 2 – Regression coefficients (rounded to nearest 0.00001) estimated for each measure and channel in the CAL condition. Bolded rows indicate cases where $R^2 \geq 0.5$.

Measure	Channel	Intercept	Age	Age^2	Sex	Age×Sex	Age^2×Sex	R^2	Age(m)	Age(f)	Age^2(m)	Age^2(f)
δ	AF7	0.43339†	-0.00152***	0.00010***	-0.03076*	0.00028	0.00010	0.210†	.	.	.	.
δ	AF8	0.42873†	-0.00201†	0.00013†	-0.03468*	0.00101	0.00009	0.280†	.	.	.	.
δ	TP9	0.95463†	-0.00312†	0.00011†	0.01803	-0.00095	0.00004	0.482†	.	.	.	.
$\boldsymbol{\delta}$	**TP10**	0.94772†	-0.00320†	0.00013†	0.02609*	-0.00074	0.00001	0.535†	.	.	.	.
θ	AF7	-0.13675†	-0.00064*	0.00007***	0.01798	0.00084	0.00013**	0.380†	-0.00064*	0.00021	0.00007***	0.00020†
θ	AF8	-0.15823†	-0.00095**	0.00008***	-0.00064	0.00091	0.00011*	0.282†	-0.00095**	-0.00004	0.00008***	0.00019†
θ	TP9	0.43667†	-0.00191†	0.00006**	0.01132	0.00025	0.00008*	0.393†	-0.00191†	-0.00166***	0.00006**	0.00013***
$\boldsymbol{\theta}$	**TP10**	0.41830†	-0.00225†	0.00009†	0.03257***	0.00018	0.00005	0.515†	.	.	.	.
$\boldsymbol{\alpha}$	**AF7**	-0.32292†	0.00090**	0.00006**	0.11225†	0.00116*	0.00009*	0.798†	0.00090***	0.00206†	0.00006***	0.00015†
$\boldsymbol{\alpha}$	**AF8**	-0.36987†	0.00071*	0.00007***	0.07154†	0.00068	0.00008*	0.645†	0.00071*	0.00139**	0.00007***	0.00016†
α	TP9	0.45606†	-0.00139†	-0.00004*	-0.01559	0.00040	0.00015***	0.229†	-0.00139***	-0.00099	-0.00004*	0.00011**
α	TP10	0.47902†	-0.00145†	-0.00000	0.00667	0.00000	0.00012*	0.228†	-0.00145***	-0.00144**	-0.00000	0.00011**
$\boldsymbol{\beta}$	**AF7**	-0.08567†	0.00242†	0.00009**	0.26647†	0.00072	0.00001	0.846†	.	.	.	.
$\boldsymbol{\beta}$	**AF8**	-0.15873†	0.00318†	0.00008**	0.20429†	-0.00027	-0.00000	0.810†	.	.	.	.
$\boldsymbol{\beta}$	**TP9**	0.34545†	0.00173†	-0.00005**	0.05945†	0.00008	0.00009*	0.608†	0.00173†	0.00181***	-0.00005**	0.00004
$\boldsymbol{\beta}$	**TP10**	0.37780†	0.00224†	-0.00000	0.07855†	-0.00085	0.00007	0.589†	.	.	.	.
$\boldsymbol{\alpha}$ **Peak**	**AF7**	10.28787†	-0.02162†	0.00010	-0.00010†	0.00122	0.00002	0.510†	.	.	.	.
α Peak	AF8	10.22824†	-0.01597†	0.00018	-0.29203***	-0.00341	0.00024	0.351†	.	.	.	.
$\boldsymbol{\alpha}$ **Peak**	**TP9**	9.57089†	-0.01469†	0.00002	0.02296	-0.00592*	-0.00010	0.584†	-0.01469†	-0.02060†	0.00002	-0.00008
$\boldsymbol{\alpha}$ **Peak**	**TP10**	9.60727†	-0.01367†	-0.00004	0.06327	-0.00426	-0.00007	0.567†	.	.	.	.
α Asym	AF8-AF7	-0.04695†	-0.00018	0.00002	-0.04071†	-0.00048	-0.00001	0.338†	.	.	.	.
α Asym	TP10-TP9	0.02296†	-0.00006	0.00004†	0.02225†	-0.00039	-0.00004	0.220†	.	.	.	.

significance levels: $* < 0.05$, $** < 0.01$, $*** < 0.001$, $\dagger < 0.0001$

Table 3 – Regression coefficients (rounded to nearest 0.00001) estimated for each measure and channel in the NFB condition. Bolded rows indicate cases where $R^2 \geq 0.5$.

Measure	Channel	Intercept	Age	Age^2	Sex	Age×Sex	Age^2×Sex	R^2	Age(m)	Age(f)	Age^2(m)	Age^2(f)
δ	AF7	0.29099†	-0.00202†	0.00013†	-0.02249	0.00133	0.00011	0.267†	·	·	·	·
δ	AF8	0.28779†	-0.00267†	0.00013†	-0.02768	0.00130	0.00012*	0.319†	-0.00267†	-0.00137	0.00013†	0.00025†
$\boldsymbol{\delta}$	**TP9**	0.76347†	-0.00388†	0.00011†	-0.00821	-0.00021	0.00006	0.620†	·	·	·	·
$\boldsymbol{\delta}$	**TP10**	0.74835†	-0.00418†	0.00014†	0.00111	0.00013	-0.00000	0.662†	·	·	·	·
θ	AF7	-0.24320†	-0.00136†	0.00008†	0.02290*	0.00207***	0.00010*	0.412†	-0.00136†	0.00071	0.00008***	0.00019†
θ	AF8	-0.26573†	-0.00146†	0.00007***	0.00793	0.00161**	0.00013**	0.365†	-0.00146†	0.00015	0.00007**	0.00021†
θ	TP9	0.35367†	-0.00196†	0.00004*	-0.02996**	0.00082	0.00014***	0.373†	-0.00196†	-0.00113*	0.00004*	0.00017†
θ	TP10	0.31149†	-0.00262†	0.00009†	-0.00430	0.00087	0.00010*	0.480†	-0.00262†	-0.00175***	0.00009†	0.00018†
$\boldsymbol{\alpha}$	**AF7**	-0.39869†	0.00123†	0.00007***	0.11474†	0.00206***	0.00008*	0.815†	0.00123†	0.00329†	0.00007***	0.00015†
$\boldsymbol{\alpha}$	**AF8**	-0.44195†	0.00101**	0.00006***	0.08223†	0.00142*	0.00010*	0.712†	0.00101**	0.00243†	0.00006**	0.00016†
α	TP9	0.48919†	0.00049	-0.00005*	-0.02840*	0.00065	0.00016**	0.105**	0.00049	0.00114	-0.00005*	0.00011**
α	TP10	0.47046†	0.00024	-0.00002	-0.00498	0.00052	0.00013**	0.087**	0.00024	0.00075	-0.00002	0.00012**
$\boldsymbol{\beta}$	**AF7**	-0.18422†	0.00197†	0.00011***	0.26647†	0.00174*	0.00004	0.868†	0.00197†	0.00372†	0.00011†	0.00015**
$\boldsymbol{\beta}$	**AF8**	-0.23850†	0.00233†	0.00008**	0.21553†	0.00046	0.00003	0.813†	·	·	·	·
$\boldsymbol{\beta}$	**TP9**	0.29314†	0.00206†	-0.00005**	0.05542†	0.00067	0.00012**	0.669†	0.00206†	0.00273†	-0.00005**	0.00006*
$\boldsymbol{\beta}$	**TP10**	0.28957†	0.00216†	0.00000	0.08575†	0.00011	0.00007	0.675†	·	·	·	·
$\boldsymbol{\alpha}$ **Peak**	**AF7**	9.72796†	-0.03847†	0.00052***	-0.03651	0.00159	-0.00028	0.779†	·	·	·	·
$\boldsymbol{\alpha}$ **Peak**	**AF8**	9.82156†	-0.03457†	0.00010	-0.05259	-0.00074	-0.00009	0.665†	·	·	·	·
$\boldsymbol{\alpha}$ **Peak**	**TP9**	9.46783†	-0.01795†	0.00001	0.11219*	-0.00647*	-0.00032	0.723†	-0.01795†	-0.02442†	0.00001	-0.00030
$\boldsymbol{\alpha}$ **Peak**	**TP10**	9.54145†	-0.01891†	-0.00000	0.06429	-0.00865***	0.00004	0.768†	-0.01891†	-0.02756†	0.00000	0.00004
α Asym	AF8-AF7	-0.04326†	-0.00022	-0.00000	-0.03251†	-0.00064	0.00002	0.235†	·	·	·	·
α Asym	TP10-TP9	-0.01873†	-0.00025	0.00004†	0.02342†	-0.00013	-0.00003	0.246†	·	·	·	·

significance levels: $* < 0.05$, $** < 0.01$, $*** < 0.001$, $\dagger < 0.0001$

3.1.1 delta (δ) power

Delta power measured at each electrode in the NFB condition is plotted as a function of age in Figure 4, and the results of the regression analyses in the CAL and NFB conditions are shown in Tables 2 and 3. In the CAL condition, the regression model accounted for statistically significant amounts of age-related variance at all electrodes, but accounted for $\geq$ 50% of age-related variance only in channel TP10 (and 48% of the variance in TP9). Similar results were obtained in the NFB condition: all of the fits accounted for statistically significant amounts of variance, but accounted for $\geq$ 50% of the variance only in the two temporoparietal channels. In both conditions, delta power decreased between 20 and 40 years of age, and then levelled off or increased slightly beyond $\approx$ 50 years of age. We also found that, in the CAL condition, the effect of Sex differed significantly from zero (TP10 $\beta = 0.02609, p = 0.02$), suggesting that delta power was slightly higher in females than males.

3.1.2 theta (θ) power

Theta (θ) power measured at each electrode in the NFB condition is plotted as a function of age in Figure 5. The figures indicate that the effects of age on theta power were qualitatively similar to those found with delta power. For example, as was the case with delta power, theta power decreased slightly between 20 and 40 years of age and increased slightly beyond 50 years of age. There also is an indication that sex differences were larger in individuals older than 60 years of age. However, a comparison of Figures 4 and 5 suggests that age-related changes in theta were smaller than age-related changes in delta. The regression results are consistent with these observations: As was found with delta power, only the regression on data from the temporoparietal channel TP10 accounted for large amounts (i.e., $\approx$ 50%) of age-related variance in theta power, and the significant effect of Sex at TP10 and the significant interactions between Sex and either Age or Age^2 in almost all cases reflect greater theta power for females than males, especially at later years. However, the best-fitting coefficients for the Age and Age^2 variables were smaller for theta power than for delta power.

3.1.3 alpha (α) power

Alpha (α) power measured at each electrode in the NFB condition is plotted as a function of age in Figure 6. A comparison of Figure 6 to Figures 4 and 5 suggests that age-related changes in alpha power differed from age-related changes in delta and theta power. For example, sex differences in alpha power, particularly at frontal electrodes, are much larger than those observed for delta and theta power. Also, unlike what was found with delta and theta power, age-related changes in alpha power appear to be greater at frontal than temporoparietal electrodes, and furthermore alpha power appears to increase, not decrease, with age. The regression analyses were consistent with these observations. In the CAL and NFB conditions, the linear models accounted for significant portions of age-related variance at all electrodes, but accounted for at least 50% of age-related variance only at AF7 and AF8. Also, the best-fitting coefficient for Age was positive at frontal sites, indicating that alpha power, unlike delta and theta power, increased with increasing age. However, the best-fitting coefficient for Age at the temporoparietal sites was slightly negative, indicating an age-related decrease in temporoparietal alpha power. The significant coefficient for Sex, indicating greater alpha power in females than males at the mean age of 42, was much greater than the effect of Sex estimated for delta and theta power. Finally, the Age and Age^2 coefficients were generally larger for females than males, indicating greater age-related changes in alpha power for females.

3.1.4 beta (β) power

Beta (β) power measured at each electrode in the NFB condition is plotted as a function of age in Figure 7. As was found with alpha power, i) there is clear evidence that beta power measured at frontal electrodes increased with age; ii) beta power was on average significantly higher in females than males; and iii) the sex difference and the trend across age were much smaller in data from temporoparietal electrodes, but unlike alpha, still highly significant (*cf.* Figures 6 & 7). The regression results in the CAL and NFB conditions generally were consistent with these observations – the coefficients for Age, Age^2, and Sex were significantly greater than zero – although the model accounted for more than 50% of the age-related variance in beta power at frontal *and* temporoparietal electrodes.

3.1.5 alpha (α) peak frequency

Alpha peak frequency in the NFB condition is plotted as a function age for each electrode in Figure 8. First, the alpha peak frequency analysis differs from the other analyses because not all participants had a clear alpha peak frequency. In fact, of the 6029 participants, approximately 88% had a peak frequency in the alpha range at the temporoparietal sites, while only 50% had an alpha peak frequency in the frontal sites. More specifically, at each channel, the following number of participants had alpha peak frequencies during the NFB session: TP9 (5374), TP10 (5379), AF7 (3085), and AF8 (2806). Similarly, the number of participants with alpha peak frequencies during the CAL session were as followed: TP9 (5136), TP10 (5320), AF7 (3111), and AF8 (2939) (note: the weights in the WLS regression models were adjusted to reflect these numbers for the alpha peak frequency analyses). Importantly, alpha peak frequencies were found for categorically more at the temporoparietal sites compared to the frontal sites, which is consistent with the grand average PSD (Figure 1) showing a clear peak in the alpha range for sites TP9 and TP10, but not for AF7 and AF8. Regardless, even after exclusion of observers without visible alpha peak frequencies, we had sufficient data to complete the analyses across the life span for each sex.

At all four electrodes, the alpha peak frequency exhibited a steady decline between 20 and 60 years of age. Compared to effects of age on the various power bands, age-related changes in alpha peak frequency exhibit a much smaller quadratic component and a much smaller difference between males and females. Regression analyses of the CAL and NFB data were consistent with these observations, though the model accounted for more age-related variance at all four electrodes in the NFB condition than the CAL condition. At temporoparietal sites, the trend across Age was significantly more negative for females than males. Also note that the effect of Age was slightly greater for alpha measured at frontal electrodes than temporoparietal electrodes (*cf.*, Tables 2 & 3).

3.2 Alpha Asymmetry

Alpha asymmetry reflects the difference between left and right alpha power, measured by subtracting the $\log_{10}$-transformed alpha power in the left hemisphere from the $\log_{10}$-transformed alpha power in the right hemisphere. The asymmetry is calculated separately at the frontal and temporoparietal sites: A negative asymmetry value reflects stronger left than right alpha power, and a positive asymmetry value reflects stronger right than left alpha power. Increased alpha power is typically associated with increased inhibition, and thus alpha power is thought to be inversely related to brain activity: Increased alpha in one hemisphere is interpreted as decreased overall activity in that hemisphere. For example a negative alpha asymmetry value typically is interpreted as showing greater neural activity in the right hemisphere relative to the left hemisphere.

Alpha asymmetry is plotted as a function of age in Figure 9. At frontal electrodes, the asymmetry was slightly negative, indicating that alpha power was relatively greater in the right than left hemisphere, and the asymmetry was more negative in females than males. At temporoparietal electrodes, the average asymmetry was slightly positive or zero, and the asymmetry was slightly more positive in females than males. Finally, at both frontal and temporoparietal sites we found little evidence for significant age-related changes in alpha asymmetry. The regression analyses were consistent with these observations: the best-fitting intercept was significantly less than zero at the frontal electrodes in the CAL and NFB conditions and significantly greater than zero at the temporoparietal electrodes in the CAL condition; in both conditions the Sex coefficient was significantly less than zero at frontal electrodes and significantly greater than zero at temporoparietal electrodes, and the effect of Age was small in all conditions. Furthermore, in all cases the model failed to account for at least 50% of the variance, again suggesting that there was very little, systematic age-related variance in alpha asymmetry.

4 Discussion

We collected frontal and temporoparietal EEG data from 6029 individuals ranging in age from 18 to 88 years while they performed a category exemplar task and a MBSR-based exercise conducted at home using the Muse headband. We investigated how EEG power in the traditional frequency bands, alpha peak frequency, and alpha asymmetry changed as a function of age and sex. Our aim was to use the powerful sample size of the data collected using the Muse to characterize both large and subtle changes in EEG dynamics.

We found that EEG power was stronger in temporoparietal than frontal leads (Figure 1). This finding was expected, given that all channels were referenced to Fpz, although temporoparietal regional power is generally higher than frontal regions (Coben et al., 2008; Dustman et al., 1993). Our findings highlight the prevalence of a sex difference in the general population, with females having higher overall EEG power in most frequency bands (Veldhuizen et al., 1993). The sex differences are consistent with previous studies demonstrating higher power in females in delta and alpha bands during sleep (Latta et al., 2005), slow waves during sleep (Mourtazaev et al., 1995), overall beta activity (Mundy-Castle, 1951), and delta, theta, alpha and beta bands during rest and during photic stimulation (Carrier et al., 2001; Wada et al., 1994). These replications of previously-reported studies suggest that valid and reliable aspects of EEG can be measured when Muse is used by consumers in an uncontrolled environment. Overall higher power in female EEG may be related to various functional and anatomical sex differences, including thicker cortical grey matter in females (Sowell et al., 2007), increased neuronal processes in females (Rabinowicz et al., 1999), and different skull thicknesses (Hagemann et al., 2008; Roche, 1953).

Power in the slow wave delta and theta bands decreased significantly with age (Figures 4 & 5), and although the decrease was slight, it is consistent with the downward trend of these slow waves observed during childhood (Matthis et al., 1980; Benninger et al., 1984; Marshall et al., 2002; Otero et al., 2003). The downward trend in delta and theta is accompanied by increased power in the alpha and beta bands (Figure 6 & 7), which has not been previously reported, but is consistent with trends observed throughout childhood (Benninger et al., 1984; Carrier et al., 2001).

Consistent with previous findings, beta power increased significantly with age and was greater in females than males (Mundy-Castle, 1951; Carrier et al., 2001). Although our methods were not designed to measure beta activation in response to a stimulus/task demands, increased beta power in older adults may be consistent with work demonstrating an association between poor attention and beta modulation (Gola et al., 2012). Increased baseline beta activity may be associated with less beta modulation overall: Training with beta neurofeedback is associated with increased attention and arousal, which is thought to explain both lower reaction times and improved sensitivity in a sustained attention task (Egner and Gruzelier, 2004). Sustained visual attention has also been linked to beta activity (Wróbel, 2000), underscoring the importance of understanding how beta activity changes with age, and whether these changes are associated with age-related changes in attention. The link between beta modulation and baseline beta activity is not yet established, but the strong age-related trend observed here suggests it may merit further investigation.

Females had significantly greater frontal alpha power than males, consistent with previous results (Latta et al., 2005). As indicated by the intercepts of the linear models, frontal alpha power was greater during CAL than NFB, suggesting a task-mediated modulation. Alpha power is known to be modulated by task demands (Payne et al., 2013), fatigue (Crabbe and Dishman, 2004), and mindfulness meditation (Kerr et al., 2011), all of which are likely at play during use of the Muse.

The strongest age-related change we saw in the data was a year-by-year slowing of the alpha peak frequency (Figure 8), which decreased similarly for males and females. This decrease was strongest at frontal sites. The slowing of alpha replicates extensive research demonstrating alpha peak frequency is age-dependent (Woodruff and Kramer, 1979; Duffy et al., 1984; Giaquinto and Nolfe, 1986; Clark et al., 2004). Alpha slowing throughout adulthood is in contrast to the increase in the alpha peak frequency during normal childhood development (Marshall et al., 2002). The shift at the two ends of the life span do not seem to be perfectly symmetrical, with changes in the adult years being very gradual compared to rapid changes throughout childhood. The age-related decline of the alpha peak frequency may be associated with reduced working memory capability (Clark et al., 2004). Using neurofeedback, Angelakis et al. (2007) demonstrated that training older adults to increase their peak alpha frequency was positively correlated with cognitive processing speed and executive function, but not with improved memory. It is also worth saying that correlations between alpha peak frequency and cognitive measures should consider the role of beta, given our earlier discussion of beta power being associated with attentional control.In our sample, there was a significant negative correlation between alpha peak frequency and beta power, where beta power increased as alpha peak frequency slowed (AF7: $r = -0.34, \beta = -0.084, p < 0.0002$, with similar results at other channels). This relation may be important because changes in beta power and alpha peak have both been independently associated with cognitive/attentional deficits, but further direct investigation is required.

We used frontal alpha asymmetry as a proxy to measure differences in relative left/right EEG activity. Participants, especially females, presented with negative frontal asymmetry during both sessions, representing greater relative right frontal activity (Davidson et al., 2000). Relatively greater right frontal activity is associated with the behavioral inhibition system (*cf.* behavioral activation system, together known as BIS/BAS), which entails a general tendency to withdraw and disengage from aversive stimuli, and a greater propensity to experience negative emotion (Sutton and Davidson, 1997), although this relation has been questioned (Coan and Allen, 2003). Also, frontal asymmetry was very similar during CAL and NFB sessions, suggesting that it is likely trait- and not state-dependent (Tomarken et al., 1992; Mathewson et al., 2015). Further analyses are required to test the stability/test-retest reliability of asymmetry during sessions with the Muse.

If asymmetry is a valid index of affective types, then the overall negative asymmetry is especially interesting given our data: Participants were consumers using a neurofeedback device to assist in mindfulness-based exercises at home. Besides early adopters likely comprising a significant portion of the current consumers (who comprise of more men than women in markets such as the USA (Ipsos, 2012; Chau and Lung Hui, 1998)), there ought to be a sizeable proportion of consumers who used the Muse specifically to improve their mental well-being. Therefore, we can expect the user-base to present with negative affect/negative asymmetry, especially given that we restricted our sample to the first five sessions per participant. InteraXon's constantly growing, updated database should be used to compare the same users after extensive meditation sessions. In fact, MBSR training with healthy older individuals has been linked to improved well-being and a reduced rightward shift in activity (Moynihan et al., 2013). Interestingly, their results suggest a normal, age-related rightward trajectory of asymmetry, with MBSR helping prevent/reduce this trajectory, which is then associated with improved well-being on several fronts, including executive and immune functions (also see Davidson et al. (2003)).

There is growing evidence linking alpha asymmetry and mindfulness, and mindfulness to enhanced physical and mental well-being. For example, mindfulness exercises can modulate somatosensory attention (Kerr et al., 2013), consistent with the view that mindfulness enhances attention to bodily sensations (Kerr et al., 2013; Kabat-Zinn, 1994). More generally, mindfulness is associated with attention regulation (Rani and Rao, 1996; Tang et al., 2007), which is tightly linked to alpha oscillations (Payne and Sekuler, 2014), suggesting that alpha-training through mindfulness may be beneficial for enhancing attentional control. Other benefits of mindfulness-based exercises include reduced emotional interference (Ortner et al., 2007) and increased regulation (Arch and Craske, 2006), lower perceived stress and increased positive affect (Nyklíček and Kuijpers, 2008; Tang et al., 2007; Carmody and Baer, 2008), reduced fatigue and anxiety (Zeidan et al., 2010), and improvements in working memory and processing fluency (Zeidan et al., 2010; Chambers et al., 2008). Future replications of EEG patterns measured in laboratory settings with data collected in the home with Muse will help us to generalize experimental results to real-world scenarios and better understand the physical and psychological benefits of mindfulness-related exercises.

In conjunction with the above discussion, it is worthwhile to be cognizant of the nature of the data and any possible issues of selection bias (Hernán et al., 2004). Although these issues are unlikely to impact our results in any significant way due to the massive sample size, the *consumer* product may have attracted individuals seeking to begin, or continue, meditation exercises. As such, the data presented here may not be entirely representative of the normal population, but rather a population of meditative individuals, or a population of individuals who share some trait that makes them more likely to be interested in meditation. The data presented here were not tagged with information regarding the users' intents and experiences with mediation, however our understanding is that InteraXon has begun to collect this data as part of a software update, allowing future researchers to address any potential issue of bias in participant selection in an updated and much larger database. Furthermore, the fact that our pattern of results are consistent with previous results found in smaller, but well-controlled, studies, increases our confidence that selection bias effects did not drive our results. As such, we focus our conclusions on the true power of this study: the enormous sample size with data points at every adult age, separately for males and females.

Overall, with increasing age there was a shift in EEG power towards higher frequency bands at the expense of the lower frequencies. Peak alpha frequency underwent a year-by-year slowing, and Muse users, especially females, exhibited relatively greater right frontal activity. We demonstrated large-scale replication of previous small-scale laboratory studies, which we see as not only a validation of these previous studies, but also as validating the Muse database and highlighting the utility of doing further, more intricate analyses using this large and perhaps more representative community-based participant database. Our primary aim was to demonstrate the utility of using such data sets to look at EEG dynamics at the population level, as they provide remarkable power to detect sex differences and gradual changes with age.

References

Angelakis, E., Stathopoulou, S., Frymiare, J. L., Green, D. L., Lubar, J. F., Kounios, J., jan 2007. EEG neurofeedback: a brief overview and an example of peak alpha frequency training for cognitive enhancement in the elderly. The Clinical neuropsychologist 21 (1), 110–29.

Arch, J. J., Craske, M. G., 2006. Mechanisms of mindfulness: Emotion regulation following a focused breathing induction. Behaviour Research and Therapy 44 (12), 1849–1858.

Benninger, C., Matthis, P., Scheffner, D., 1984. EEG development of healthy boys and girls. Results of a longitudinal study. Electroencephalography and Clinical Neurophysiology 57 (1), 1–12.

Carmody, J., Baer, R. A., 2008. Relationships between mindfulness practice and levels of mindfulness, medical and psychological symptoms and well-being in a mindfulness-based stress reduction program. Journal of Behavioral Medicine 31 (1), 23–33.

Carrier, J., Land, S., Buysse, D. J., Kupfer, D. J., Monk, T. H., 2001. The effects of age and gender on sleep EEG power spectral density in the middle years of life (ages 20-60 years old). Psychophysiology 38 (2), 232–42.

Chambers, R., Lo, B. C. Y., Allen, N. B., 2008. The impact of intensive mindfulness training on attentional control, cognitive style, and affect. Cognitive Therapy and Research 32 (3), 303–322.

Chau, P. Y., Lung Hui, K., 1998. Identifying early adopters of new IT products: A case of Windows 95. Information & Management 33, 225–230.

Clark, C. R., Veltmeyer, M. D., Hamilton, R. J., Simms, E., Paul, R., Hermens, D., Gordon, E., jun 2004. Spontaneous alpha peak frequency predicts working memory performance across the age span. International Journal of Psychophysiology 53 (1), 1–9.

Coan, J. a., Allen, J. J. B., 2003. Frontal EEG asymmetry and the behavioral activation and inhibition systems. Psychophysiology 40 (1), 106–114.

Coben, R., Clarke, A. R., Hudspeth, W., Barry, R. J., 2008. EEG power and coherence in autistic spectrum disorder. Clinical Neurophysiology 119 (5), 1002–1009.

Crabbe, J. B., Dishman, R. K., 2004. Brain electrocortical activity during and after exercise: A quantitative synthesis. Psychophysiology 41 (4), 563–574.

Davidson, R. J., Jackson, D. C., Larson, C. L., 2000. Human electroencephalography. In: Cacioppo, J. T., Tassinary, L. G., Bernston, G. G. (Eds.), Handbook of psychophysiology, 2nd Edition. Cambridge University Press, Ch. 2, pp. 27–52.

Davidson, R. J., Kabat-Zinn, J., Schumacher, J., Rosenkranz, M., Muller, D., Santorelli, S. F., Urbanowski, F., Harrington, A., Bonus, K., Sheridan, J. F., 2003. Alterations in brain and immune function produced by mindfulness meditation. Psychosomatic Medicine 65 (4), 564–570.

Duffy, F. H., Albert, M. S., McAnulty, G., Garvey, A. J., 1984. Age-related differences in brain electrical activity of healthy subjects. Annals of Neurology 16 (4), 430–438.

Dustman, R., Shearer, D., Emmerson, R., 1993. EEG and event-related potentials in normal aging. Progress in neurobiology.

Egner, T., Gruzelier, J. H., 2004. EEG Biofeedback of low beta band components: Frequency-specific effects on variables of attention and event-related brain potentials. Clinical Neurophysiology 115 (1), 131–139.

Giaquinto, S., Nolfe, G., 1986. The EEG in the normal elderly: a contribution to the interpretation of aging and dementia. Electroencephalography and clinical . . . 63 (6), 540–546.

Gola, M., Kamiński, J., Brzezicka, A., Wróbel, A., 2012. ?eta Band Oscillations As a Correlate of Alertness–Changes in Aging. International Journal of Psychophysiology 85 (1), 62–7.

Hagemann, D., Hewig, J., Walter, C., Naumann, E., 2008. Skull thickness and magnitude of EEG alpha activity. Clinical Neurophysiology 119 (6), 1271–1280.

Hernán, M. A., Hernandez-Diaz, S., Robins, J. M., 2004. A structural approach to selection bias. Epidemiology 15 (5), 615–625.

Hintze, J. L., Nelson, R. D., 1998. Violin plots: A box plot-density trace synergism. American Statistician 52 (2), 181–184.

Ipsos, 2012. Socialogue: Me First, Me First! Tech. Rep. November, Ipsos. URL http://www.ipsos-na.com/news-polls/pressrelease.aspx?id=5888

Kabat-Zinn, J., 1994. Mindfulness meditation for everyday life. Piatkus Books, London.

Kabat-Zinn, J., 2003. Mindfulness-based interventions in context: Past, present, and future. Clinical Psychology: Science and Practice 10 (2), 144–156.

Kerr, C. E., Jones, S. R., Wan, Q., Pritchett, D. L., Wasserman, R. H., Wexler, A., Villanueva, J. J., Shaw, J. R., Lazar, S. W., Kaptchuk, T. J., Littenberg, R., Hämäläinen, M. S., Moore, C. I., 2011. Effects of mindfulness meditation training on anticipatory alpha modulation in primary somatosensory cortex. Brain Research Bulletin 85 (3-4), 96–103.

Kerr, C. E., Sacchet, M. D., Lazar, S. W., Moore, C. I., Jones, S. R., 2013. Mindfulness starts with the body: somatosensory attention and top-down modulation of cortical alpha rhythms in mindfulness meditation. Frontiers in human neuroscience 7 (February), 12.

Latta, F., Leproult, R., Tasali, E., Hofmann, E., Van Cauter, E., 2005. Sex differences in delta and alpha EEG activities in healthy older adults. Sleep 28 (12), 1525–1534.

Marshall, P. J., Bar-Haim, Y., Fox, N. A., 2002. Development of the EEG from 5 months to 4 years of age. Clinical Neurophysiology 113 (8), 1199–1208.

Mathewson, K. J., Hashemi, A., Sheng, B., Sekuler, A. B., Bennett, P. J., Schmidt, L. A., 2015. Regional electroencephalogram (EEG) alpha power and asymmetry in older adults: a study of short-term test?retest reliability. Frontiers in aging neuroscience 7 (177), 1–10.

Matthis, P., Scheffner, D., Benninger, C., Lipinski, C., Stolzis, L., 1980. Changes in the background activity of the electroencephalogram according to age. Electroencephalography and Clinical Neurophysiology 49 (5-6), 626–635.

Mourtazaev, M. S., Kemp, B., Zwinderman, a. H., Kamphuisen, H. a., 1995. Age and gender affect different characteristics of slow waves in the sleep EEG. Sleep 18 (7), 557–564.

Moynihan, J. a., Chapman, B. P., Klorman, R., Krasner, M. S., Duberstein, P. R., Brown, K. W., Talbot, N. L., 2013. Mindfulness-based stress reduction for older adults: Effects on executive function, frontal alpha asymmetry and immune function. Neuropsychobiology 68 (1), 34–43.

Mundy-Castle, A., 1951. Theta and beta rhythm in the electroencephalograms of normal adults. Electroencephalography and clinical neurophysiology 3 (4), 477–486.

Nyklíček, I., Kuijpers, K. F., 2008. Effects of mindfulness-based stress reduction intervention on psychological well-being and quality of life: Is increased mindfulness indeed the mechanism? Annals of Behavioral Medicine 35 (3), 331–340.

Ortner, C. N. M., Kilner, S. J., Zelazo, P. D., 2007. Mindfulness meditation and reduced emotional interference on a cognitive task. Motivation and Emotion 31 (4), 271–283.

Otero, G. A., Pliego-Rivero, F. B., Fernández, T., Ricardo, J., 2003. EEG development in children with sociocultural disadvantages: A follow-up study. Clinical Neurophysiology 114 (10), 1918–1925.

Payne, L., Guillory, S., Sekuler, R., 2013. Attention-modulated alpha-band oscillations protect against intrusion of irrelevant information. Journal of cognitive neuroscience, 1463–1476.

Payne, L., Sekuler, R., 2014. The importance of ignoring: alpha oscillations protect selectivity. Current Directions in Psychological Science 23 (3), 171–177.

Rabinowicz, T., Dean, D. E., Petetot, J. M., de Courten-Myers, G. M., 1999. Gender differences in the human cerebral cortex: more neurons in males; more processes in females. Journal of child neurology 14 (2), 98–107.

Rani, N. J., Rao, P. V. K., 1996. Meditation and attention regulation. Journal of Indian Psychology 14 (1-2), 26–30.

Roche, A. F., 1953. Increase in cranial thickness during growth. Human biology; an international record of research 25 (2), 81–92.

Sowell, E. R., Peterson, B. S., Kan, E., Woods, R. P., Yoshii, J., Bansal, R., Xu, D., Zhu, H., Thompson, P. M., Toga, A. W., 2007. Sex differences in cortical thickness mapped in 176 healthy individuals between 7 and 87 years of age. Cerebral Cortex 17 (7), 1550–1560.

Sutton, S. K., Davidson, R. J., 1997. Prefrontal brain asymmetry: A biological substrate of the behavioural approach and inhibition systems. Psychological science 8 (3), 204–210.

Tang, Y.-Y., Ma, Y., Wang, J., Fan, Y., Feng, S., Lu, Q., Yu, Q., Sui, D., Rothbart, M. K., Fan, M., Posner, M. I., 2007. Short-term meditation training improves attention and self-regulation. Proceedings of the National Academy of Sciences of the United States of America 104 (43), 17152–17156.

Tomarken, a. J., Davidson, R. J., Wheeler, R. E., Kinney, L., 1992. Psychometric properties of resting anterior EEG asymmetry: temporal stability and internal consistency. Psychophysiology 29 (5), 576–592.

Veldhuizen, R. J., Jonkman, E. J., Poortvliet, D. C., 1993. Sex differences in age regression parameters of healthy adults–normative data and practical implications. Electroencephalography and clinical neurophysiology 86 (6), 377–384.

Wada, Y., Takizawa, Y., Zheng-Yan, J., Yamaguchi, N., apr 1994. Gender Differences in Quantitative EEG at Rest and during Photic Stimulation in Normal Young Adults. Clinical EEG and Neuroscience 25 (2), 81–85.

Woodruff, D. S., Kramer, D. a., 1979. EEG alpha slowing, refractory period, and reaction time in aging. Experimental aging research 5 (4), 279–292.

Wróbel, A., 2000. Beta activity: A carrier for visual attention. Acta Neurobiologiae Experimentalis 60 (2), 247–260.

Zeidan, F., Johnson, S. K., Diamond, B. J., David, Z., Goolkasian, P., 2010. Mindfulness meditation improves cognition: Evidence of brief mental training. Consciousness and Cognition 19 (2), 597–605.

Figure Captions

Figure 1. Average power spectra, at each channel for CAL (left) and NFB (right) conditions. Frontal and temporoparietal channels are represented by black and grey lines, respectively, and left and right channels in these regions are represented by solid and dashed lines, respectively.

Figure 2. Log_{10}-transformed EEG power in the 0-30 Hz range measured in females (white) and males (grey) at each channel for NFB (left) and CAL (right), shown in the form of violin plots (Hintze and Nelson, 1998). Filled circles represent the median, and the first and third quartiles are identified by the bottom and top of the bold vertical lines, respectively. The bottom and top of the thin vertical line represents the lower and upper adjacent values, respectively. Females had slightly higher power at all channels, regardless of task.

Figure 3. Standard deviation of the average band power across ages (x-axis) plotted with the average standard deviation of each band power across participants within each age (y-axis). Within age SD was calculated by calculating the SD across participants at each given age. Ages 78 and above all had 2 or fewer participants, so we grouped them into a single age bin. Mean within age SD (y-axis) was calculated as the average within age SD. Between age SD (x-axis) was calculated by first computing the mean band power for each individual age, then calculating the SD across these values.

Figure 4. Delta (δ) band power plotted against age for males (grey symbols) and females (white symbols). Each point represents the mean for that age; symbol size represents how many individuals were used to compute the mean. Regression was used to compute the best-fitting curves separately for males (solid line) and females (dashed line), and the shaded regions represents 95% confidence intervals.

Figure 5. Theta (θ) band power plotted against age for males (grey symbols) and females (white symbols). Each point represents the mean for that age; symbol size represents how many individuals were used to compute the mean. Regression was used to compute the best-fitting curves separately for males and females, and the shaded regions represents 95% confidence intervals.

Figure 6. Alpha (α) band power plotted against age for males (grey symbols) and females (white symbols). Each point represents the mean for that age; symbol size represents how many individuals were used to compute the mean. Regression was used to compute the best-fitting curves separately for males and females, and the shaded regions represents 95% confidence intervals.

Figure 7. Beta (β) band power plotted against age for males (grey symbols) and females (white symbols). Each point represents the mean for that age; symbol size represents how many individuals were used to compute the mean. Regression was used to compute the best-fitting curves separately for males and females, and the shaded regions represents 95% confidence intervals.

Figure 8. Alpha peak frequency plotted against age for males (grey symbols) and females (white symbols). Each point represents the mean for that age; symbol size represents how many individuals were used to compute the mean. Regression was used to compute the best-fitting curves separately for males and females, and the shaded regions represents 95% confidence intervals.

Figure 9. Alpha asymmetry measured at frontal (top) and temporoparietal (bottom) electrodes plotted against age for males (grey symbols) and females (white symbols). Each point represents the mean for that age; symbol size represents how many individuals were used to compute the mean. Regression was used to compute the best-fitting curves separately for males and females, and the shaded regions represents 95% confidence intervals.

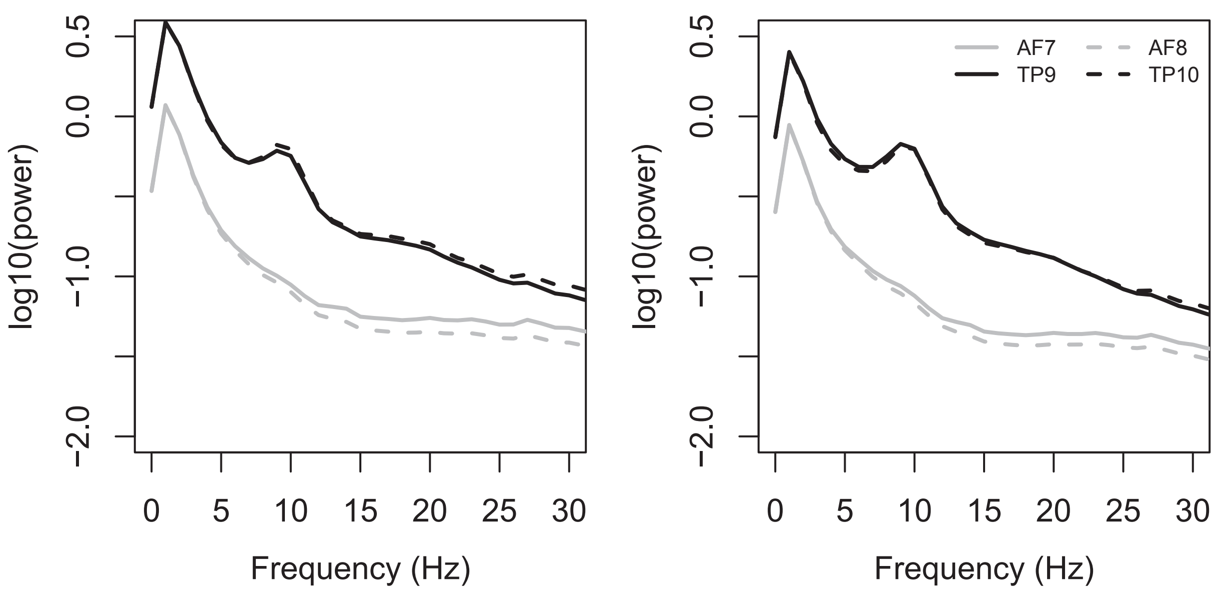

log10(power)
0.5
0.0
−1.0
−2.0
0
5
10
15
20
25
30
Frequency (Hz)
AF7
AF8
TP9
TP10

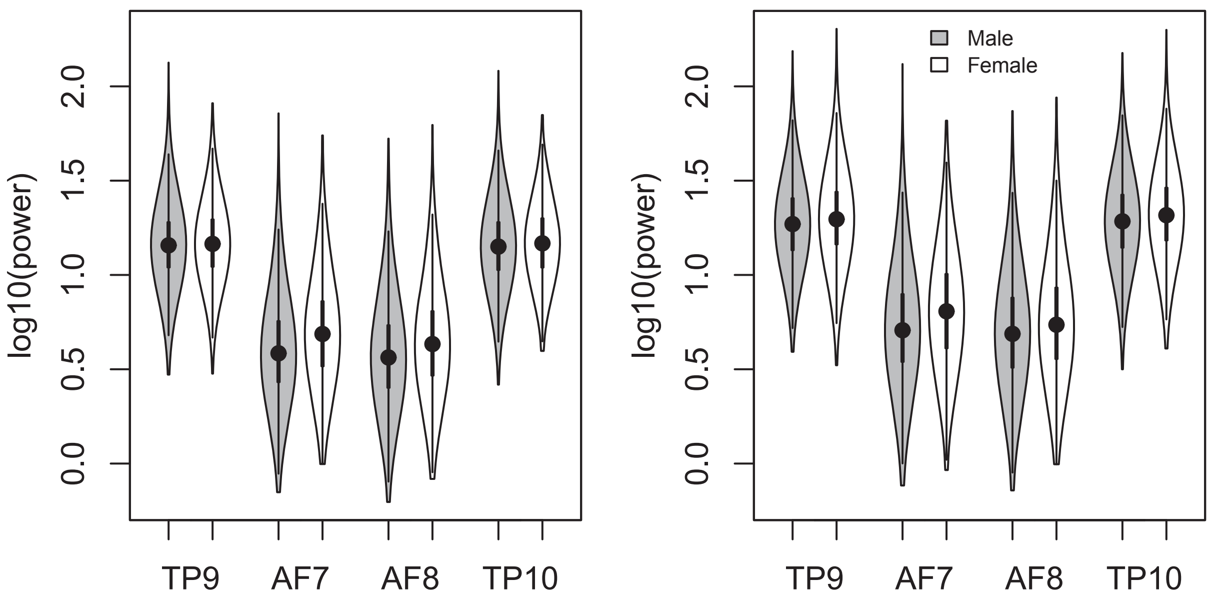
log10(power)
0.0
0.5
1.0
1.5
2.0
TP9
AF7
AF8
TP10
log10(power)
0.0
0.5
1.0
1.5
2.0
Male
Female
TP9
AF7
AF8
TP10

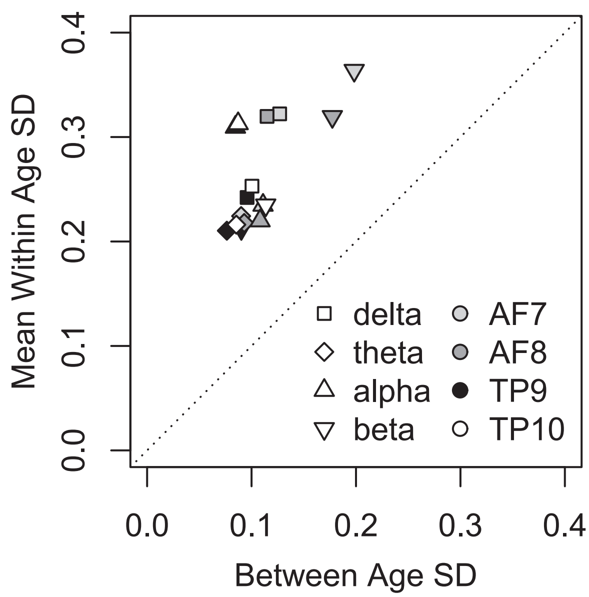

Mean Within Age SD
Between Age SD
0.0
0.1
0.2
0.3
0.4
delta
theta
alpha
beta
AF7
AF8
TP9
TP10

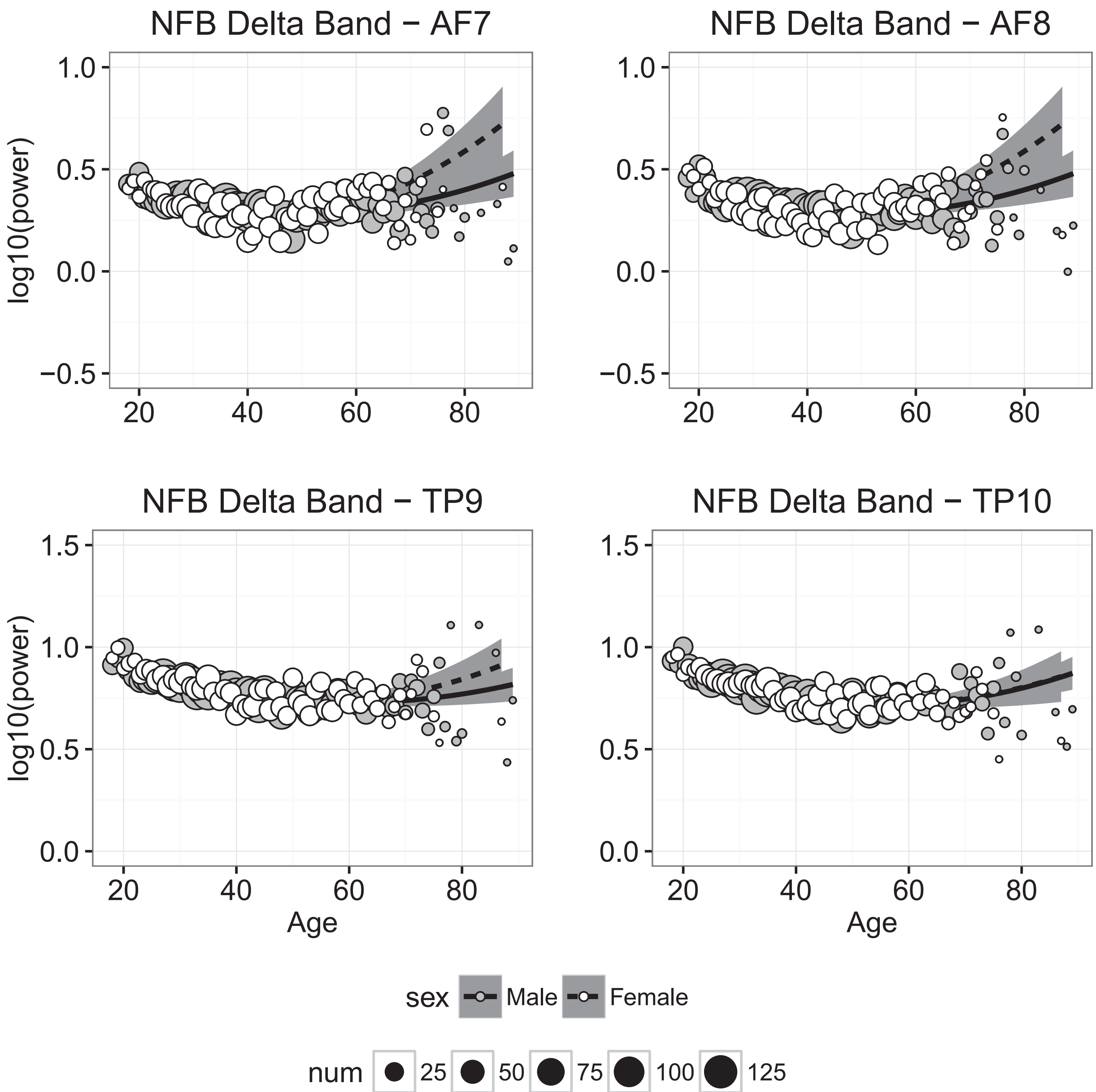

NFB Delta Band − AF7
NFB Delta Band − AF8
NFB Delta Band − TP9
NFB Delta Band − TP10
log10(power)
Age
sex
Male
Female
num
25
50
75
100
125

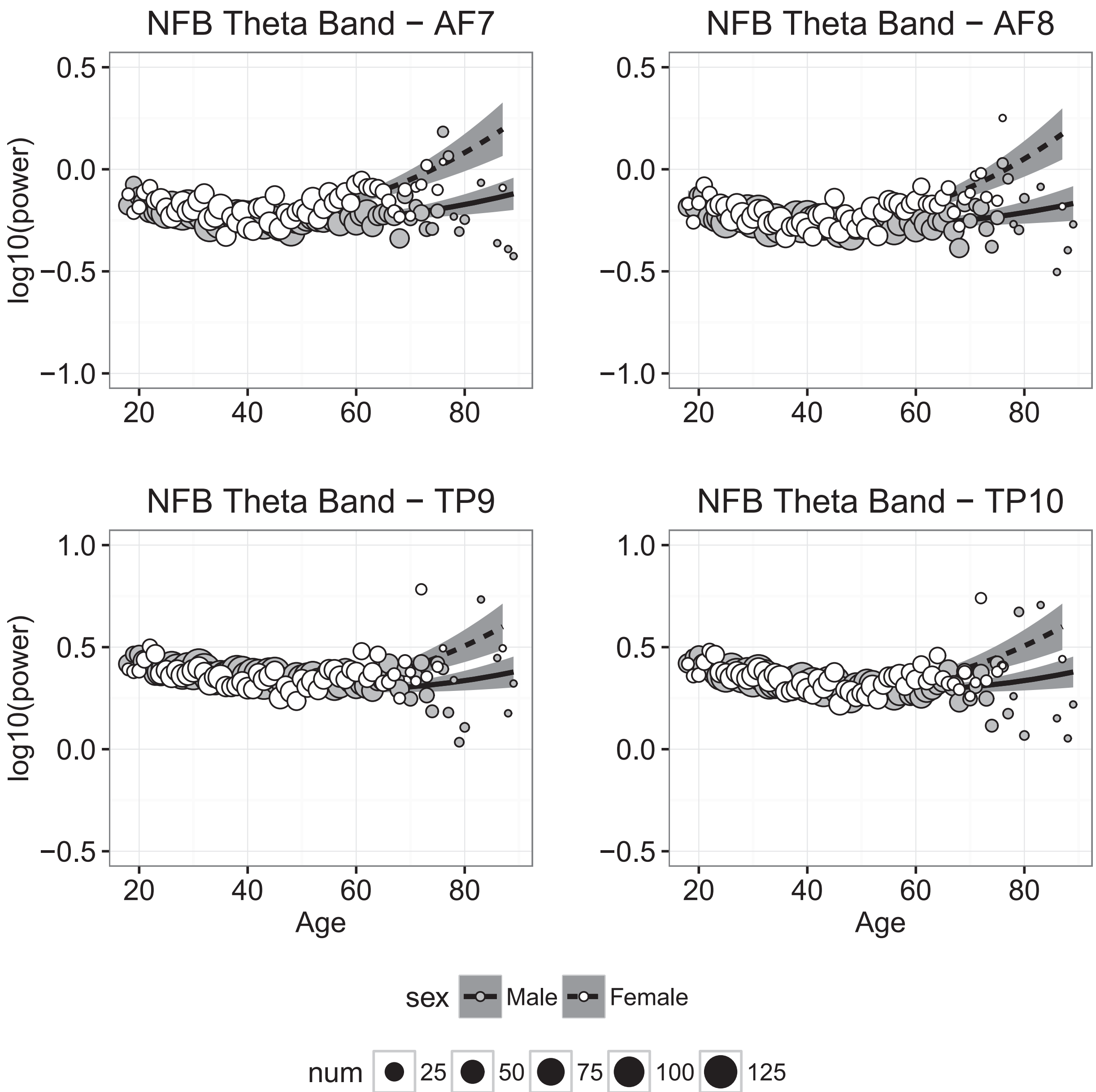
NFB Theta Band − AF7
NFB Theta Band − AF8
NFB Theta Band − TP9
NFB Theta Band − TP10
log10(power)
Age
sex
Male
Female
num
25
50
75
100
125

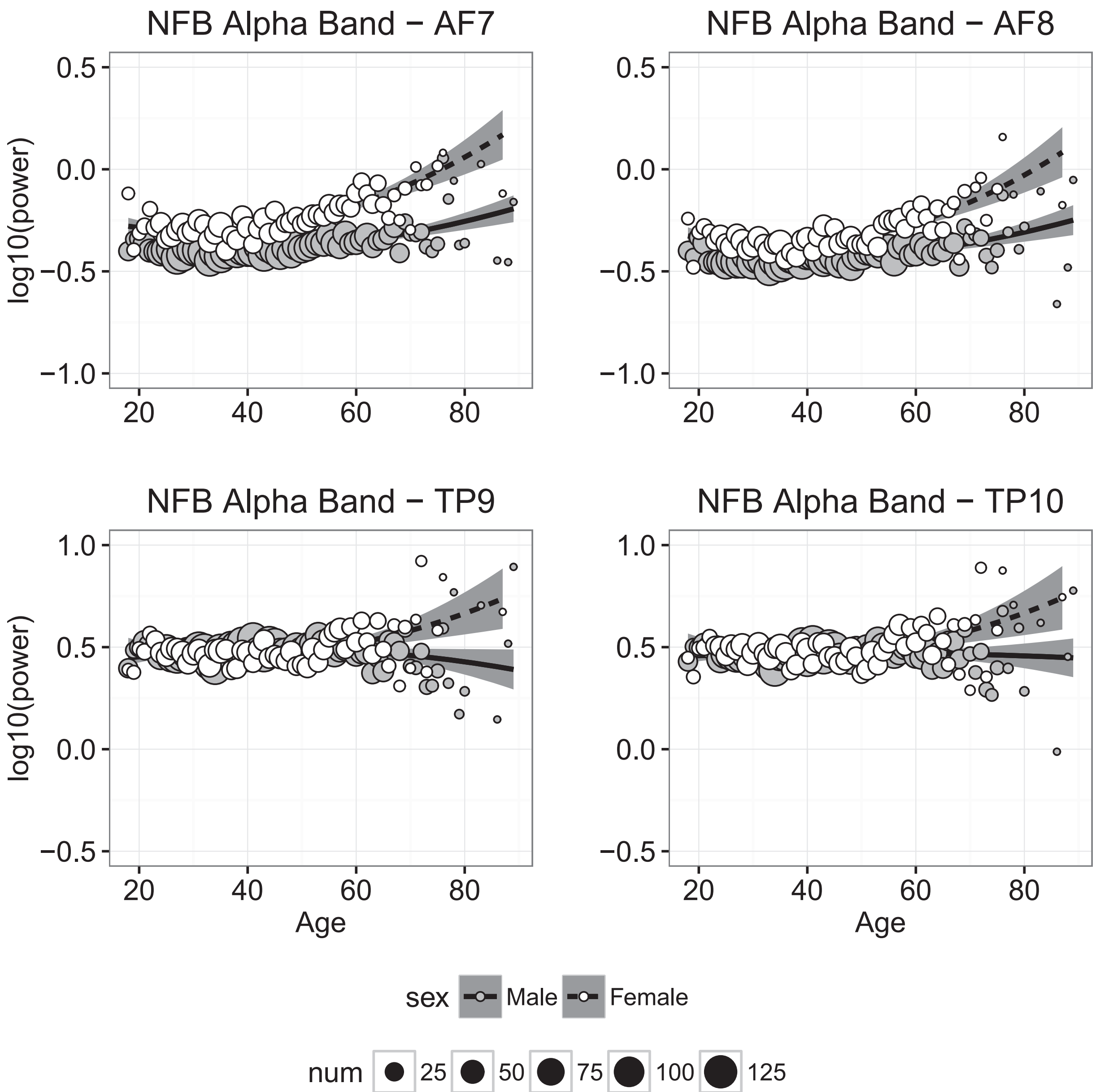

NFB Alpha Band − AF7
NFB Alpha Band − AF8
NFB Alpha Band − TP9
NFB Alpha Band − TP10
log10(power)
Age
0.5
0.0
−0.5
−1.0
1.0
20
40
60
80
sex
Male
Female
num
25
50
75
100
125

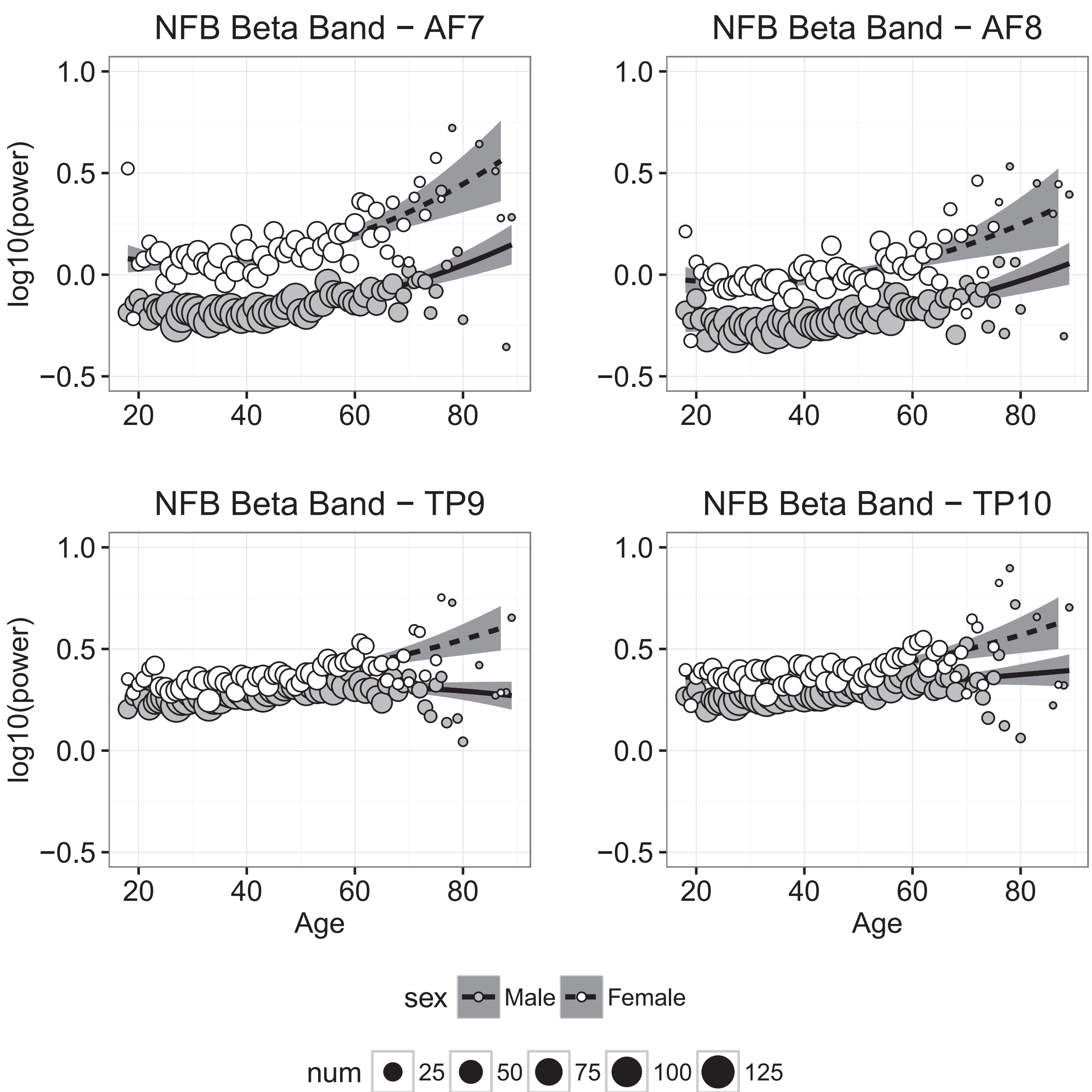
NFB Beta Band − AF7
NFB Beta Band − AF8
NFB Beta Band − TP9
NFB Beta Band − TP10
log10(power)
1.0
0.5
0.0
−0.5
20
40
60
80
Age
sex
Male
Female
num
25
50
75
100
125

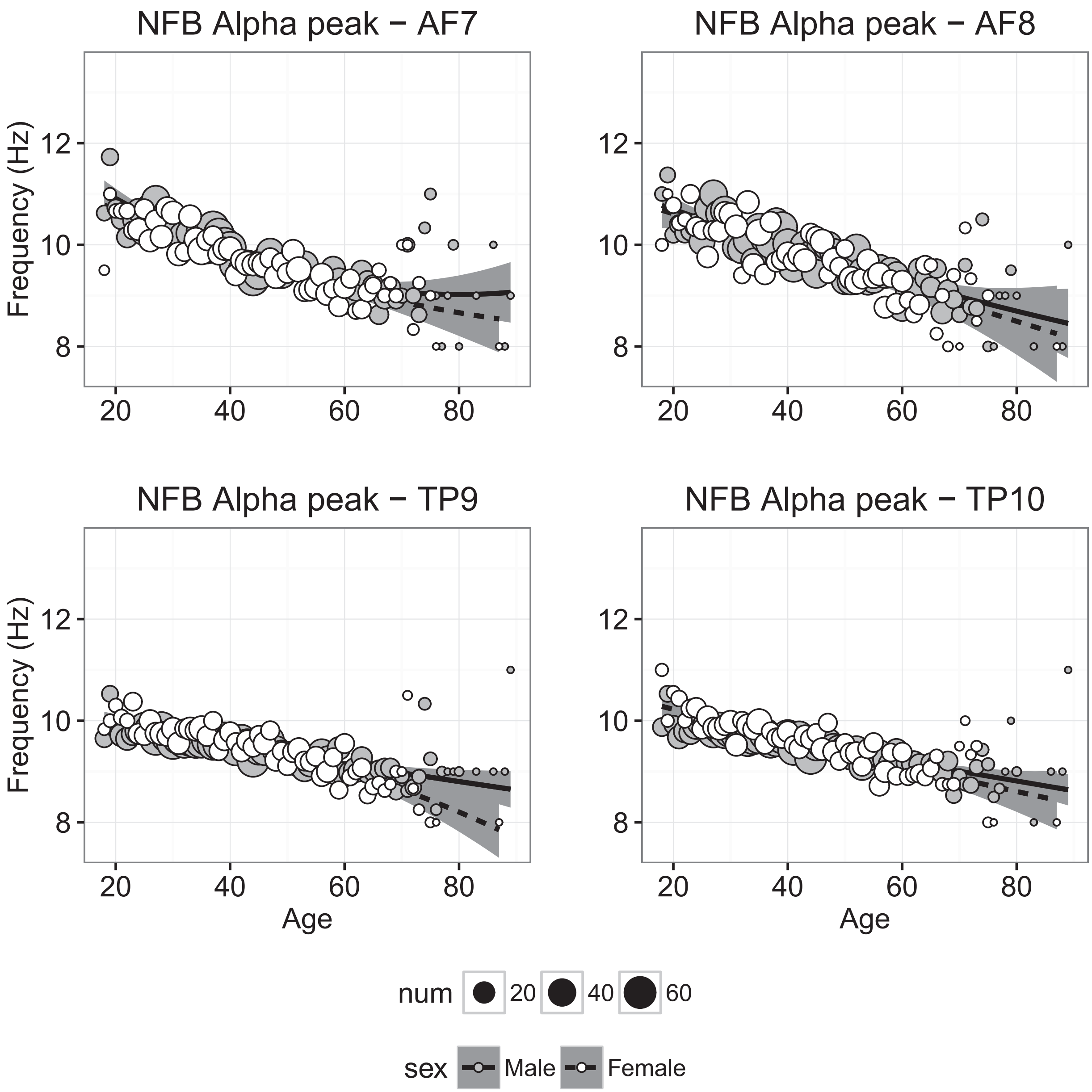
NFB Alpha peak − AF7
NFB Alpha peak − AF8
NFB Alpha peak − TP9
NFB Alpha peak − TP10
Frequency (Hz)
Age
num 20 40 60
sex Male Female

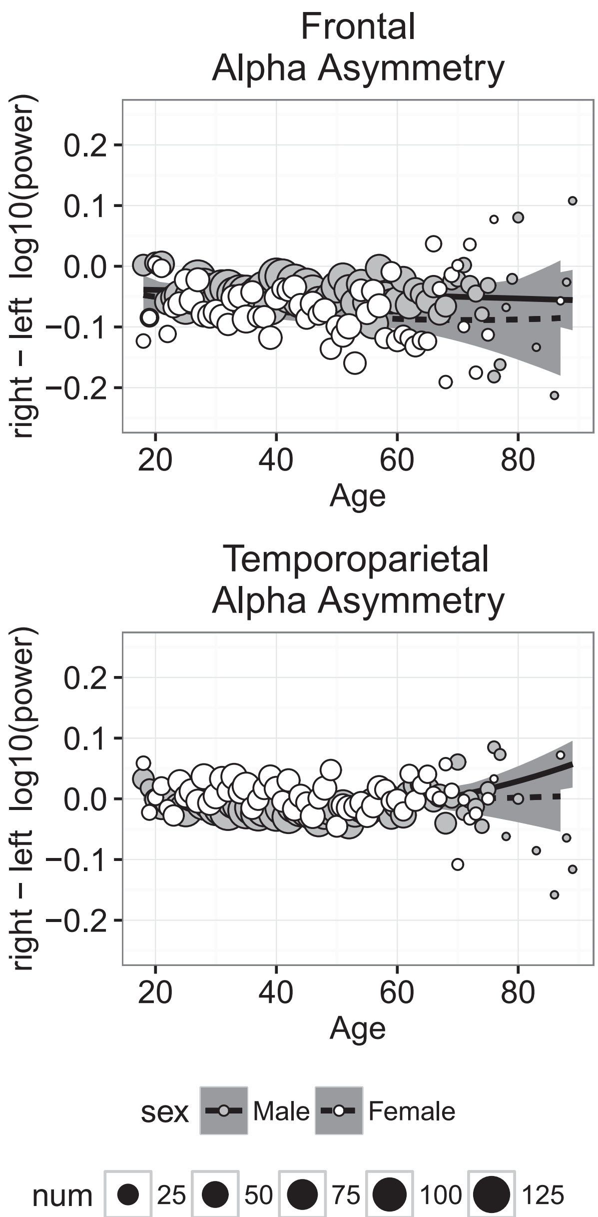
Frontal
Alpha Asymmetry
right – left log10(power)
0.2
0.1
0.0
−0.1
−0.2
20
40
60
80
Age
Temporoparietal
Alpha Asymmetry
right – left log10(power)
0.2
0.1
0.0
−0.1
−0.2
20
40
60
80
Age
sex
Male
Female
num
25
50
75
100
125